

Research Article



The effects of bone density and crestal cortical bone thickness on micromotion and peri-implant bone strain distribution in an immediately loaded implant: a nonlinear finite element analysis

Tsutomu Sugiura,^{1*} Kazuhiko Yamamoto,¹ Satoshi Horita,¹ Kazuhiro Murakami,¹ Sadami Tsutsumi,² Tadaaki Kirita¹

¹Department of Oral and Maxillofacial Surgery, Nara Medical University, Nara, Japan

²Applied Electronics Laboratory, Kanazawa Institute of Technology, Tokyo, Japan



Received: Apr 30, 2016

Accepted: Jun 9, 2016

*Correspondence to

Tsutomu Sugiura

Department of Oral and Maxillofacial Surgery,
Nara Medical University, 840 Shijo-cho,
Kashihara City, Nara 634-8522, Japan.
E-mail: sugiurat@naramed-u.ac.jp
Tel: +81-744-29-8876
Fax: +81-744-29-8876

Copyright © 2016 Korean Academy of
Periodontology

This is an Open Access article distributed
under the terms of the Creative Commons
Attribution Non-Commercial License (<http://creativecommons.org/licenses/by-nc/3.0/>).

ORCID

Tsutomu Sugiura
<http://orcid.org/0000-0001-9601-9248>
Kazuhiro Yamamoto
<http://orcid.org/0000-0002-9931-889X>
Satoshi Horita
<http://orcid.org/0000-0002-1061-1986>
Kazuhiro Murakami
<http://orcid.org/0000-0002-2144-5020>
Sadami Tsutsumi
<http://orcid.org/0000-0002-0672-5892>
Tadaaki Kirita
<http://orcid.org/0000-0002-6900-0397>

ABSTRACT

Purpose: This study investigated the effects of bone density and crestal cortical bone thickness at the implant-placement site on micromotion (relative displacement between the implant and bone) and the peri-implant bone strain distribution under immediate-loading conditions.

Methods: A three-dimensional finite element model of the posterior mandible with an implant was constructed. Various bone parameters were simulated, including low or high cancellous bone density, low or high crestal cortical bone density, and crestal cortical bone thicknesses ranging from 0.5 to 2.5 mm. Delayed- and immediate-loading conditions were simulated. A buccolingual oblique load of 200 N was applied to the top of the abutment.

Results: The maximum extent of micromotion was approximately 100 μ m in the low-density cancellous bone models, whereas it was under 30 μ m in the high-density cancellous bone models. Crestal cortical bone thickness significantly affected the maximum micromotion in the low-density cancellous bone models. The minimum principal strain in the peri-implant cortical bone was affected by the density of the crestal cortical bone and cancellous bone to the same degree for both delayed and immediate loading. In the low-density cancellous bone models under immediate loading, the minimum principal strain in the peri-implant cortical bone decreased with an increase in crestal cortical bone thickness.

Conclusions: Cancellous bone density may be a critical factor for avoiding excessive micromotion in immediately loaded implants. Crestal cortical bone thickness significantly affected the maximum extent of micromotion and peri-implant bone strain in simulations of low-density cancellous bone under immediate loading.

Keywords: Bone density; Dental implants; Finite element analysis

Funding

This work was supported by a Grant-in Aid for Scientific Research from the Japan Society for Promotion of Science (No. 24592963).

Conflict of Interest

No potential conflict of interest relevant to this article was reported.

INTRODUCTION

Osseointegrated dental implants are widely used for functional and aesthetic rehabilitation. Conventional implants are loaded after a long period of healing. Although this approach has proven to be highly predictable and successful, the extended treatment period may be perceived as a considerable inconvenience by patients desiring rapid rehabilitation. Immediate loading has been proposed to reduce the cost and duration of the implant treatment [1], and it has shown a clinical success rate of over 95% [2].

Despite reports of promising results in experimental and clinical studies of immediate-loading protocols, failures can still occur and have been suggested to arise from biomechanical factors [3]. For example, excessive micromotion may lead to encapsulation of the implants, resulting in the failure of osseointegration between the bone and implant. Even for implants that have already become osseointegrated, the accumulation of excessive stress and strain can cause microdamage to accumulate, inducing bone resorption [4,5].

Primary stability has been characterized as one of the most important variables affecting the success of immediately loaded implants. Excessive micromotion (relative displacement between the implant and bone) may cause osseointegration to fail between the bone and implant [4,6]. The design of the implant, the quantity and density of bone, and the insertion torque influence primary stability. Studies have reported correlations of bone quantity and bone density with primary implant stability using measurements of insertion torque, removal torque, cutting torque, Periotest values (PTV), and the implant stability quotient (ISQ) derived from resonance frequency analysis [7-12]. However, every bone parameter, including cancellous bone density, cortical bone density, and cortical bone thickness, has an influence on primary stability. Moreover, most of the above measuring techniques are either low-sensitivity or show somewhat questionable correlations with other techniques [13,14]. Thus, the relative importance of bone parameters remains controversial [10,13,15].

In addition, a key factor for the success of both delayed-loading and immediately loaded implants is the manner in which the stresses and strains are transmitted to the surrounding bone. Bone density is important for the success rate of implants, because it influences the transmission of loads to implants and bone, and a high failure rate for delayed-loading implants has been reported in areas with low bone density [16]. Therefore, the effects of bone quantity and density on the peri-implant distribution of stress and strain have been investigated under delayed-loading situations [17-19]. Poor bone quantity and density also have been identified as risk factors with implications for the immediate loading of implants [20]. However, the effects of bone quantity and density on biomechanical behavior have not been yet clarified quantitatively for immediately loaded implants.

Clinically, it is impossible to introduce any device into the bone-implant interface to investigate the level of micromotion between the bone and implant under masticatory forces. Finite element analysis (FEA) is an efficient technique of evaluating both the extent of micromotion and the distribution of peri-implant bone strain. The purpose of this study was to investigate the effects of bone density at the implant-placement site on micromotion and the peri-implant bone strain distribution under immediate-loading conditions.

MATERIALS AND METHODS

Finite element models

The three-dimensional (3D) geometry of the right posterior mandible was obtained from the computed tomography (CT) scan data of a 62-year-old male, using FEA software (Mechanical Finder, Version 6.2, Research Center of Computational Mechanics, Tokyo, Japan). The cortical bone comprised the crestal, lateral, and inferior cortical bones. The cortical bone of the buccal, lingual, and inferior border of the mandible was reconstructed with a thickness of 2.5 mm [19]. Crestal cortical bone thickness at the implant placement site of the mandible ranges from approximately 0.4 mm to 2.8 mm [10,12,19]. In previous FEA studies simulating bone types based on the Lekholm and Zarb classification [21], crestal cortical bone thicknesses of 1 mm and 2 mm have been characterized as thin and thick, respectively [22]. Based on previous biomechanical studies [8,13], crestal cortical bone thicknesses of 0.5 mm, 1.0 mm, 2.0 mm, and 2.5 mm were simulated in the present study.

A Straumann threaded implant (Institut Straumann, Waldenburg, Switzerland) with a diameter of 4.1 mm and a length of 10 mm was simulated in this study. An implant and a 6-mm abutment were modeled as one piece using 3D modeling software and exported into the FEA software to complete the models (Figure 1). In the study, two conditions of the implant-bone interface (a bonded interface and a contact interface) were constructed. For delayed-loading implant models, the implant was assumed to achieve complete osseointegration at the implant-bone interface. For immediately loaded implant models, contact interfaces (non-osseointegration) between the implant and bone were simulated. The friction coefficient was set to 0.3 [3]. The material properties were assumed to be

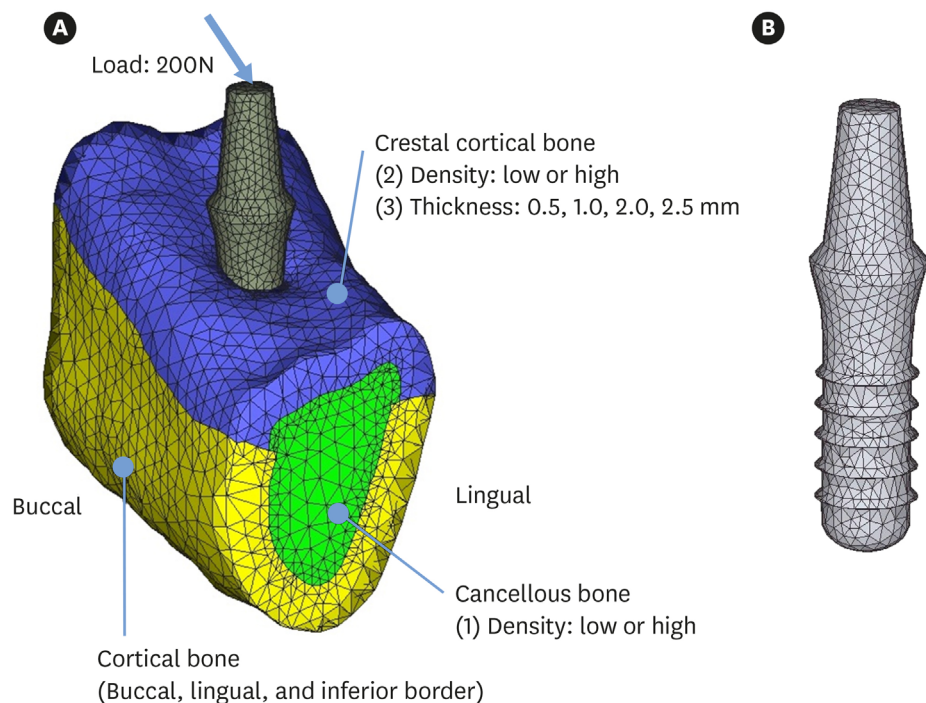


Figure 1. Finite element model. (A) The right posterior mandible model consisted of cancellous bone and cortical bone. The cortical bone comprised the crestal cortical bone and the buccal, lingual, and inferior borders of the mandible. The three independent parameters included: (1) the density of cancellous bone, (2) the density of crestal cortical bone, and (3) the thickness of crestal cortical bone. (B) Implant and abutment.

Table 1. Bone density and material properties

Material	CT value (HU)	Bone density (g/cm ³)	Young's modulus (GPa)	Poisson's ratio
Titanium			110	0.35
Cortical bone				
Alveolar crest				
Low density	950	0.639	4.14	0.30
High density	1,750	1.168	13.94	0.30
Buccal, lingual, and lower borders	1,765	1.178	14.18	0.30
Standard model			13.70	0.30
Cancellous bone				
Low density	150	0.109	0.259	0.30
High density	850	0.572	3.507	0.30
Standard model			1.37	0.30

homogeneous, isotropic, and linearly elastic. The finite element model was constructed with 4-node tetrahedral elements, and had approximately 102,000 elements and 19,000 nodes.

Definition of bone density and material properties

A detailed description of the measurement and definition of bone density has been published earlier [19]. The bone densities of 75 potential implant sites in the posterior mandible of 34 patients were measured using a spiral CT machine. The results of Kolmogorov-Smirnov tests showed that the densities of the cancellous bone and crestal cortical bone had normal statistical distributions. We defined the 5th and 95th percentiles of bone density (150 Hounsfield units [HU] and 850 HU for the cancellous bone, and 950 HU and 1750 HU for the crestal cortical bone) as low and high, respectively. Since the cortical bone densities of the buccal, lingual, and inferior border of the mandible showed similar values, the mean value (1765 HU) was used as the bone density of these areas. A linear regression equation was created based on the CT values of the calibration phantom. Using these calibrated CT data, each CT value was converted to apparent bone density expressed in g/cm³. Young's modulus for apparent bone density was calculated using the equations proposed by Keyak (Table 1) [23].

Young's modulus for the cancellous bone and cortical bone of the mandible has been frequently assumed to be 1,370 MPa and 13,700 MPa, respectively [3,24]. Thus, a model having these Young's moduli was prepared as the standard model. Poisson's ratio of bones and the material property of the titanium implant was obtained from previous data (Table 1) [24]. All experimental procedures were conducted with the ethical approval of Nara Medical University.

Loads and constraints

With fixed prostheses supported by implants, the average maximum occlusal force was approximately 200 N for the first premolar and molars [25]. A buccolingual oblique load of 200 N was applied to the top of the abutment to simulate the average maximum occlusal load and direction on the first premolar tooth (Figure 1). The loading angle was defined as 30° to the axis of the implant [26]. The boundary conditions were established by the nodes of the mesial and distal end of the model in all directions.

Analysis of micromotion and bone strain

Analyses were performed to calculate the micromotion at the bone-implant interface in the immediate-loading models, as well as the minimum principal strain around the implants. The micromotion was computed as the relative displacement between two nodes (one node on the bone side and one node on the implant side) of elements on the interface. The minimum principal strain (third principal strain) represented the most negative strain,

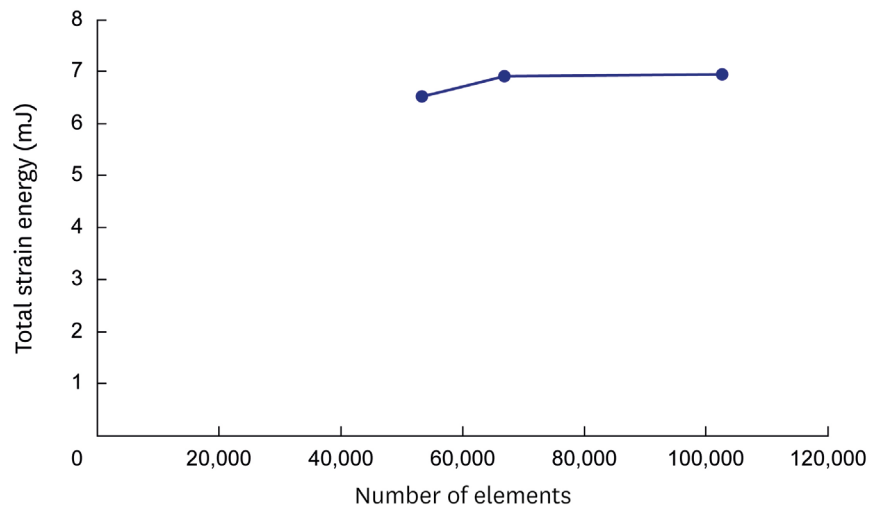


Figure 2. The results of convergence tests in the standard model with 1.0-mm crestal cortical bone under delayed loading.

typically the peak compressive strain. In order to evaluate the minimum principal strain, eight 1-mm spheres were placed at the alveolar crest around the implant in a similar manner as described in a previous report [27]. The mean value of the minimum principal strain in multiple solid elements contained in the sphere was used as the typical strain value. The absolute maximum value in these spheres was used as the peak strain value of the model.

Convergence test

A convergence test of the finite element models was performed to verify the mesh quality, and the convergence criterion was set to be less than 1% in changes of the total strain energy of all elements (Figure 2). Based on the results of the convergence test, an average element size of 0.6 mm was set for meshing in all finite element models.

RESULTS

Micromotion

In the low-density cancellous bone models, the implant was displaced lingually at the neck and buccally at the apex of the implant. In the high-density cancellous bone models, the implant was less displaced at the apex than at the neck of the implant (Figure 3). Consequently, the maximum micromotion was observed at the apex of the implant in the low-density cancellous bone models, whereas it was observed at the implant neck in the high-density cancellous bone models.

The maximum micromotion was affected more by the cancellous bone density than by the crestal cortical bone density. The maximum micromotion values in the low-density cancellous bone models were 2.8-5.5-fold higher than those in the high-density cancellous bone models. The maximum micromotion values in the low-density crestal cortical bone models were 1.2-2.0-fold higher than those in the high-density crestal cortical bone models. The greatest extent of micromotion was approximately 100 μm in the low-density cancellous bone models, whereas it was less than 30 μm in the high-density cancellous bone models. Crestal cortical bone thickness greatly affected the maximum micromotion in the low-

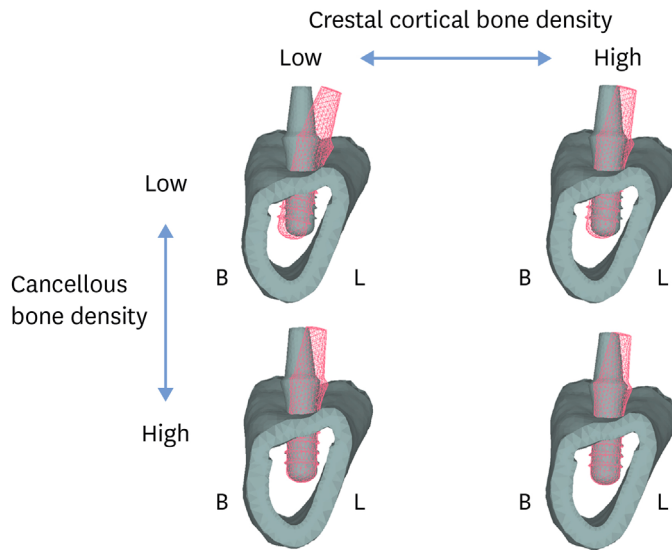


Figure 3. Displacement of the implant and abutment in the immediate-loading models with 2.0-mm crestal cortical bone. The cortical bone and the implant and abutment before deformation are also illustrated. Displacement of the implant and abutment is represented at 15× magnification in all models. B, buccal; L, lingual.

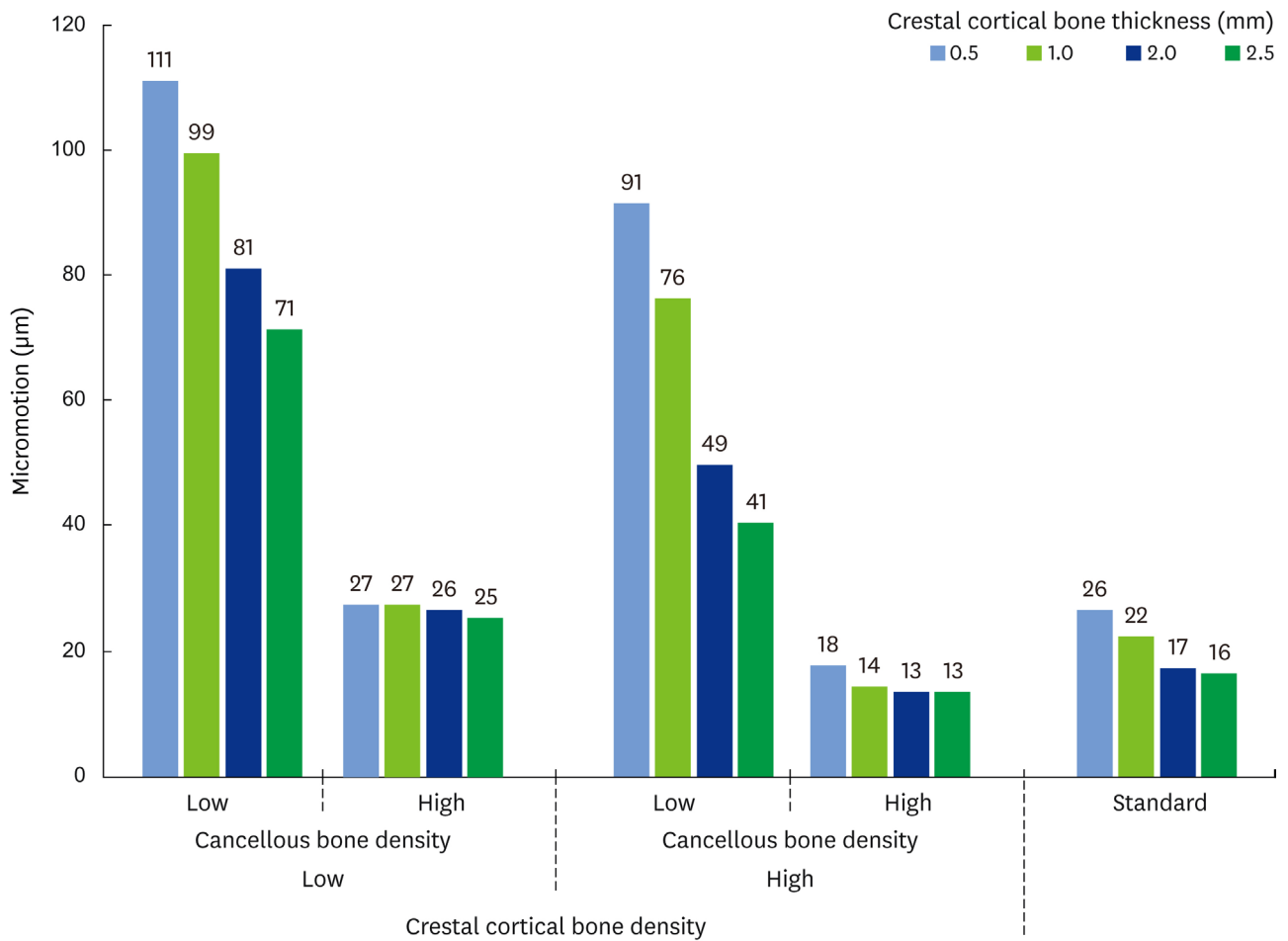


Figure 4. Maximum micromotion in the immediate-loading models.

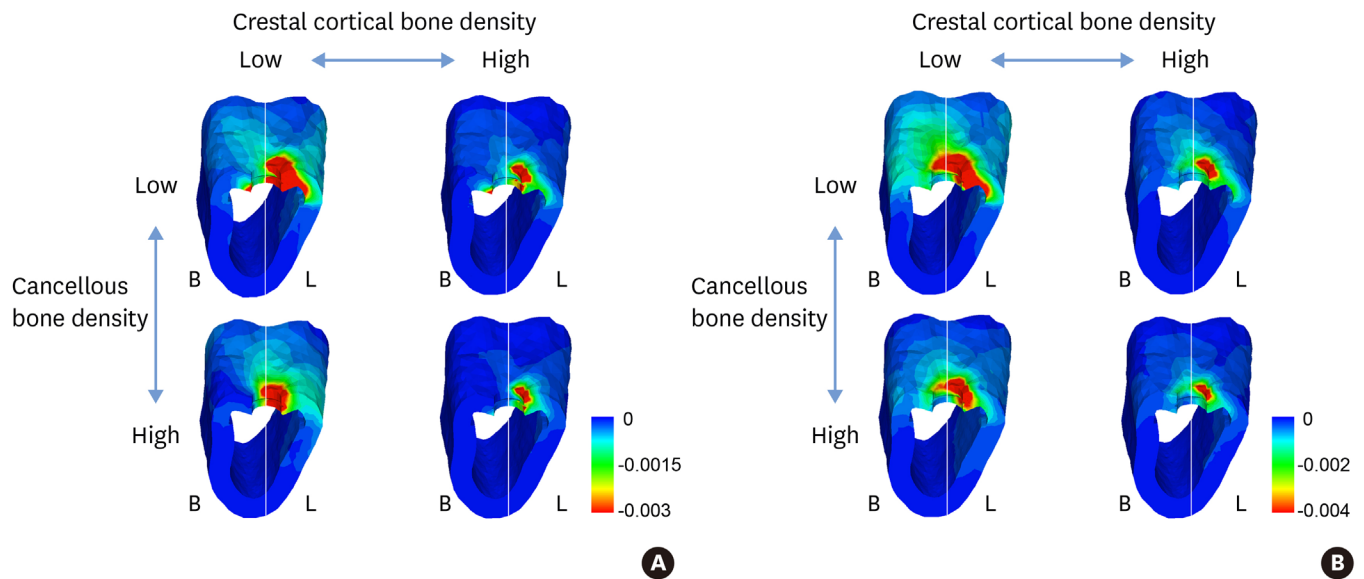


Figure 5. Minimum principal strain distribution in the cortical bone in 2.0-mm crestal cortical bone models. (A) Delayed loading. (B) Immediate loading. B, buccal; L, lingual.

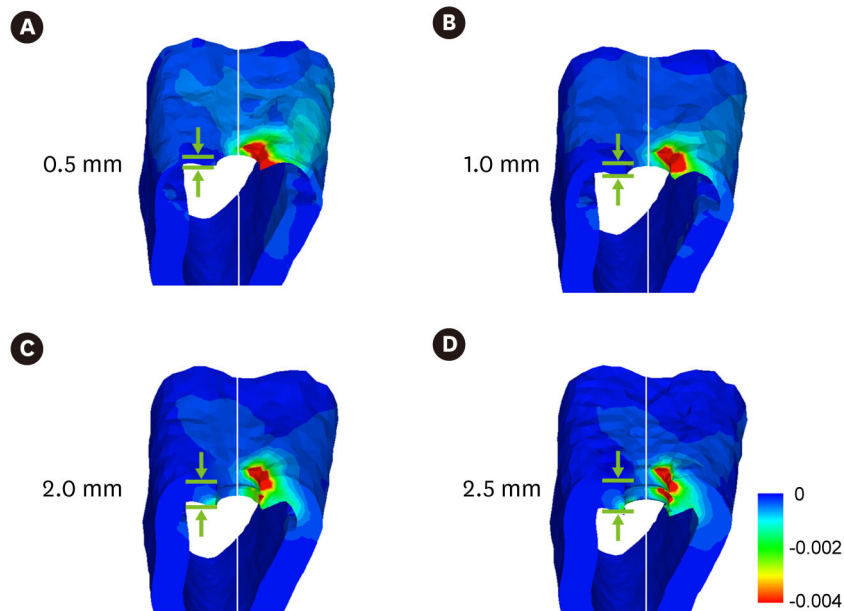


Figure 6. The effect of crestal cortical bone thickness on the minimum principal strain distribution in the cortical bone in the standard model under immediate loading. (A) 0.5 mm of thickness. (B) 1.0 mm of thickness. (C) 2.0 mm of thickness. (D) 2.5 mm of thickness. Similar trends in the minimum principal strain distributions were observed in the delayed-loading models, although the strain levels were different (data not shown).

density cancellous bone models, whereas it did not affect the maximum micromotion in the high-density cancellous bone models. In the standard models, the maximum micromotion decreased by 15.4%-38.5% with increases in the crestal bone cortical thickness, but only to 26 μm (Figure 4).

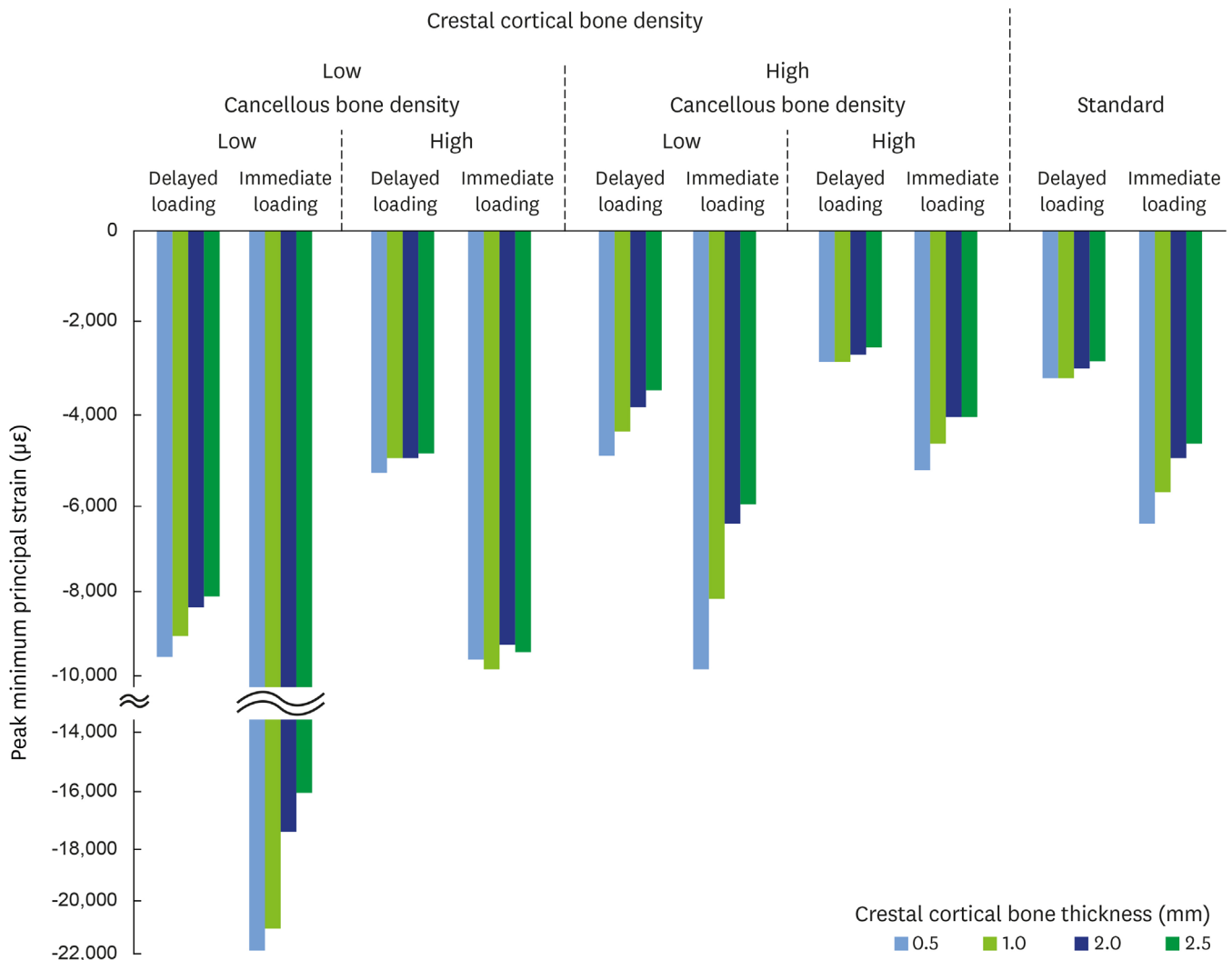


Figure 7. The peak values of minimum principal strains in the peri-implant cortical bone.

Strain distribution in the bone around the implant

The minimum principal strain concentration was located at the lingual crestal cortical bone in all models for both delayed and immediate loading (Figure 5 and 6). The peak minimum principal strain values in the immediate-loading models were 1.51-2.34-fold higher than those in the delayed-loading models (1.61-1.98-fold in the standard models). The minimum principal strain values were affected by the density of the cancellous bone and the crestal cortical bone to the same degree for both delayed and immediate loading. The peak minimum principal strain values in the low-density bone models were higher than those in the high-density bone models, by 1.35-1.84-fold in the delayed-loading model and 1.46-2.30-fold in the immediate-loading model regarding cancellous bone density, and 1.73-2.28-fold in the delayed-loading model and 1.88-2.63-fold in the immediate-loading model regarding crestal cortical bone density (Figure 7).

In the low-density cancellous bone models, the minimum principal strain decreased with an increase in the crestal cortical bone thickness. This tendency was particularly notable under immediate loading in comparison with delayed loading. In contrast, in the high-density

cancellous bone models, the peak minimum principal strain values did not significantly depend upon crestal cortical bone thickness (Figure 7).

In the standard model, the peak minimum principal strain decreased by 9.4%-26.0% with increases in crestal cortical bone thickness under immediate loading, whereas it was not affected by crestal cortical bone thickness under delayed loading (Figure 6 and 7).

DISCUSSION

Primary implant stability is essential for the successful formation of bone tissue at the bone-implant interface. The success of dental implants is not related to the timing of loading, but rather to the critical function of micromotion [4]. Micromotion of more than 150 μm can induce the formation of fibrous connective tissue, preventing the osseointegration of an immediately loaded implant [4,6]. In contrast, Vandamme et al. [28], in a bone chamber experiment, demonstrated that displacement of an implant between 30 μm and 90 μm stimulated bone formation at the implant surface. Therefore, a micromotion level from 100 μm to 150 μm may be the maximum threshold.

We found the maximum extent of micromotion to be significantly influenced by cancellous bone density. The maximum micromotion in the low-density cancellous bone models reached around 100 μm . In contrast, in the high-density cancellous bone, the maximum micromotion values were less than 30 μm . These results indicate that cancellous bone density may be a critical factor for avoiding excessive micromotion in immediately loaded implants.

A correlation between bone density and primary implant stability has been reported in previous studies. Bone density influences the ISQ [11,13,15], PTV [11,15], and insertion torque value (ITV) [8,15]. Ikumi and Tsutsumi [9] showed a significant correlation between bone density obtained by CT and cutting torque values. An *in vitro* study found that implant displacement in soft bone was significantly higher than in normal or hard bone [29]. Previous studies have also reported significant correlations between cortical bone thickness and implant stability. Increasing the crestal cortical bone thickness has been found to increase the values of the ISQ [10-12] and the ITV [15], as well as to reduce the PTV [11]. For example, Miyamoto et al. [12] found a significant correlation between the ISQ and crestal cortical bone thickness. Several *in vitro* studies using artificial bone models have shown a correlation between crestal cortical bone thickness and primary stability [7,11,13].

Studies employing FEA have shown that, when a lateral or oblique force is applied to the implant, most of the force is concentrated on the cortical bone [24]. For this reason, previous studies have focused on the anatomic background related to cortical bone thickness rather than bone density [15,30]. Several studies have demonstrated no correlations between bone density and implant stability. In one study, 22 implants were inserted into the maxillae and mandibles of human cadavers, and no correlations were found between the ISQ and histomorphometric parameters of cancellous bone analyzed using micro-CT [10]. Similarly, Nkenke et al. [14] demonstrated the importance of cortical bone thickness rather than bone density in implant stability. However, Marquezan et al. [15] showed that cancellous bone played an important role in primary stability in the presence and in the absence of cortical bone based on an analysis of histomorphometric bone parameters using bovine bone blocks.

An in vitro study using biomechanical test materials for implant stability showed the absence of correlations among methods such as resonance frequency analysis, removal torque, and axial testing [13]. Hsu et al. [11] found that initial stability was influenced by both the crestal cortical bone thickness and the Young's modulus of cancellous bone using artificial bone, but these factors were mostly nonlinearly correlated with the ITV, PTV, and ISQ. Such nonlinear relationships among bone parameters and implant stability, as well as variations in bone density and cortical bone thickness measured in clinical studies or established using biomechanical tests, may be responsible for the different interpretations presented in previous studies.

In the present study, crestal cortical bone thickness affected the maximum micromotion in the standard model and in the low-density cancellous bone models, in agreement with previous studies measuring the ITV, PTV, and ISQ [7,10-12]. However, even in the standard model, the maximum micromotion values were much less than 100 μm . Therefore, we believe that crestal cortical bone thickness plays an important role in reducing micromotion, only when the cancellous bone density is low.

Minimum principal strains were calculated for the cortical bone around the implant. Since stress and strain may induce the form of marginal bone loss known as saucerization, the stresses and strains of the crestal cortical bone adjacent to the implant neck must play a major role in the analysis [24,31]. Potential fatigue damage of the bone occurs with excessive dynamic loading that exceeds 4,000 $\mu\epsilon$ in compression and 2,500 $\mu\epsilon$ in tension [32,33]. In particular, bone resorption under compressive strain is attributed to the accumulation of induced microdamage that exceeds the capacity of the bone for repair [4,26,32]. Therefore, the minimum principal strain values in the peri-implant cortical bone were evaluated in this study.

The distributions of the minimum principal strain in the delayed and immediate-loading models were consistent with previous reports, which have shown the concentration of stress and strain to be on the compressive side [26,34]. In the immediately loaded implants, greater stress and strain develop in the cortical bone and cancellous bone because only compressive and frictional forces are transferred via the contact interfaces, compared with the bonded interfaces of the delayed implants [35]. The results of the present study agree with the findings reported by Ferreira et al. [36], who showed that the minimum principal stress in the peri-implant bone in an immediate-loading model was approximately twofold higher than was observed in a delayed-loading model.

As bone density affects peri-implant bone stress and strain in delayed-loading conditions [17,18], the minimum principal strain values in the peri-implant cortical bone under immediate loading were also affected by the density of the cancellous and crestal cortical bone. The effects of crestal cortical bone thickness on peri-implant bone stress and strain also have been investigated under delayed-loading conditions. Crestal cortical bone thickness has either a minimal effect or no effect on peri-implant bone stress and strain [18,31]. Our results are consistent with those findings in the delayed-loading models. However, in the present FEA, even in the standard model under immediate loading, the minimum principal strain was affected by crestal cortical bone thickness. In the low-density cancellous bone models, the crestal cortical bone thickness affected the peak minimum principal strain values to a greater extent. This is most likely because crestal cortical bone bears a greater load on the compression side under immediate loading than under delayed loading.

The peak minimum principal strain exceeded 4,000 $\mu\epsilon$ for all immediate-loading models. However, this does not necessarily imply bone overloading and implant loss, because in addition to strain amplitude, loading frequency and the number of loading cycles can have a significant effect on the adaptive response of cortical bone [3,5,32]. Nonetheless, the results of the present study biomechanically confirm that low-density bone and thin crestal cortical bone at the implant placement site are risk factors for overloads of immediate-loading implants, as well as providing quantitative evidence to support pre-existing recommendations in the implant community. Clinically, in immediate-loading protocols, it is emphasized that implants should be placed in areas of “good-quality” bone (types 1-3 according to the Lekholm and Zarb classification) [38] or at sites where only good primary stability is achieved [2]. Selecting implant placement sites in this way may reduce micromotion and peri-implant strain, resulting in high survival rates for immediately loaded implants.

Biomechanical evaluations of dental implants using FEA have been performed by many researchers. The validity of the simulations depends on morphology, material properties, boundary conditions, and the bone-implant interface. The most important factors in the outcome are the material properties of the materials used, such as Young’s modulus and Poisson’s ratio [39]. Therefore, we defined the degree of bone density and range of crestal cortical bone thickness using the CT data of preoperative patients [19]. This enabled us to evaluate the effects of bone parameters quantitatively.

Chang et al. [40] analyzed micromotion in an immediately loaded implant model similar to that in the present study, with a vertical load of 300 N. They showed a maximum micromotion of 8.5 μm to 15.0 μm in the model with a cortical bone thickness of 2 mm. The maximum micromotion of the standard model with 2.0-mm crestal cortical bone thickness in the present study was 17 μm . This microstrain value is also compatible with the value found by Huang et al. [35], who reported that the maximum micromotion in the high-density cancellous model was 7.9 μm , under a 30-degree oblique load of 129 N. Although the model geometry, material properties, and boundary and loading conditions were not identical, the results of this study were similar to those of other FEA studies; hence, the model of this study should be considered to have been validated accurately by previously published reports.

This finite element model had limitations, such as homogeneities and the isotropic linear elasticity of the material properties. Altering the mandibular properties with the anisotropic assumption may result in different strain distributions [35]. The load was applied in a fixed direction. The boundary conditions were set as fixed, so they did not accurately reproduce the complex forces exerted during chewing. These assumptions do not completely reflect clinical scenarios. Thus, the values of strain and micromotion could not be directly compared with clinical threshold values. Furthermore, the threshold value for micromotion may be influenced by the implant surface treatment. Nonetheless, in agreement with other quantitative studies [3,17,35-37], the present assumptions can be accepted, in a computational sense, to assess the biomechanical behavior of implants. The above limitations should be considered when applying our results to clinical situations.

In conclusion, cancellous bone density may be a critical factor for avoiding excessive micromotion in immediately loaded implants. Crestal cortical bone thickness greatly influenced the maximum micromotion only when the cancellous bone density was low. In cases with low-density cancellous bone, the minimum principal strain in the peri-implant

bone was more sensitive to changes in the crestal cortical bone thickness under immediate loading than under delayed loading.

REFERENCES

1. Misch CE, Wang HL, Misch CM, Sharawy M, Lemons J, Judy KW. Rationale for the application of immediate load in implant dentistry: Part I. *Implant Dent* 2004;13:207-17.
[PUBMED](#) | [CROSSREF](#)
2. Laviv A, Levin L, Usiel Y, Schwartz-Arad D. Survival of immediately provisionalized dental implants: a case-control study with up to 5 years follow-up. *Clin Implant Dent Relat Res* 2010;12 Suppl 1:e23-7.
[PUBMED](#) | [CROSSREF](#)
3. Pessoa RS, Coelho PG, Muraru L, Marcantonio E Jr, Vaz LG, Vander Sloten J, et al. Influence of implant design on the biomechanical environment of immediately placed implants: computed tomography-based nonlinear three-dimensional finite element analysis. *Int J Oral Maxillofac Implants* 2011;26:1279-87.
[PUBMED](#)
4. Brunski JB, Puleo DA, Nanci A. Biomaterials and biomechanics of oral and maxillofacial implants: current status and future developments. *Int J Oral Maxillofac Implants* 2000;15:15-46.
[PUBMED](#)
5. Duyck J, Rønold HJ, Van Oosterwyck H, Naert I, Vander Sloten J, Ellingsen JE. The influence of static and dynamic loading on marginal bone reactions around osseointegrated implants: an animal experimental study. *Clin Oral Implants Res* 2001;12:207-18.
[PUBMED](#) | [CROSSREF](#)
6. Pilliar RM, Lee JM, Maniopoulos C. Observations on the effect of movement on bone ingrowth into porous-surfaced implants. *Clin Orthop Relat Res* 1986;(208):108-13.
[PUBMED](#)
7. Tabassum A, Meijer GJ, Wolke JG, Jansen JA. Influence of surgical technique and surface roughness on the primary stability of an implant in artificial bone with different cortical thickness: a laboratory study. *Clin Oral Implants Res* 2010;21:213-20.
[PUBMED](#) | [CROSSREF](#)
8. Bayarchimeg D, Namgoong H, Kim BK, Kim MD, Kim S, Kim TI, et al. Evaluation of the correlation between insertion torque and primary stability of dental implants using a block bone test. *J Periodontal Implant Sci* 2013;43:30-6.
[PUBMED](#) | [CROSSREF](#)
9. Ikumi N, Tsutsumi S. Assessment of correlation between computerized tomography values of the bone and cutting torque values at implant placement: a clinical study. *Int J Oral Maxillofac Implants* 2005;20:253-60.
[PUBMED](#)
10. Rozé J, Babu S, Saffarzadeh A, Gayet-Delacroix M, Hoornaert A, Layrolle P. Correlating implant stability to bone structure. *Clin Oral Implants Res* 2009;20:1140-5.
[PUBMED](#) | [CROSSREF](#)
11. Hsu JT, Fuh LJ, Tu MG, Li YF, Chen KT, Huang HL. The effects of cortical bone thickness and trabecular bone strength on noninvasive measures of the implant primary stability using synthetic bone models. *Clin Implant Dent Relat Res* 2013;15:251-61.
[PUBMED](#) | [CROSSREF](#)
12. Miyamoto I, Tsuboi Y, Wada E, Suwa H, Iizuka T. Influence of cortical bone thickness and implant length on implant stability at the time of surgery--clinical, prospective, biomechanical, and imaging study. *Bone* 2005;37:776-80.
[PUBMED](#) | [CROSSREF](#)
13. Bardin T, Gédet P, Hallermann W, Büchler P. Quantifying the influence of bone density and thickness on resonance frequency analysis: an in vitro study of biomechanical test materials. *Int J Oral Maxillofac Implants* 2009;24:1006-14.
[PUBMED](#)
14. Nkenke E, Hahn M, Weinzierl K, Radespiel-Tröger M, Neukam FW, Engelke K. Implant stability and histomorphometry: a correlation study in human cadavers using stepped cylinder implants. *Clin Oral Implants Res* 2003;14:601-9.
[PUBMED](#) | [CROSSREF](#)

15. Marquezan M, Lima I, Lopes RT, Sant'Anna EF, de Souza MM. Is trabecular bone related to primary stability of miniscrews? *Angle Orthod* 2014;84:500-7.
[PUBMED](#) | [CROSSREF](#)
16. Palma-Carrió C, Maestre-Ferrín L, Peñarrocha-Oltra D, Peñarrocha-Diago MA, Peñarrocha-Diago M. Risk factors associated with early failure of dental implants. A literature review. *Med Oral Patol Oral Cir Bucal* 2011;16:e514-7.
[PUBMED](#) | [CROSSREF](#)
17. Petrie CS, Williams JL. Probabilistic analysis of peri-implant strain predictions as influenced by uncertainties in bone properties and occlusal forces. *Clin Oral Implants Res* 2007;18:611-9.
[PUBMED](#) | [CROSSREF](#)
18. Guan H, van Staden R, Loo YC, Johnson N, Ivanovski S, Meredith N. Influence of bone and dental implant parameters on stress distribution in the mandible: a finite element study. *Int J Oral Maxillofac Implants* 2009;24:866-76.
[PUBMED](#)
19. Sugiura T, Yamamoto K, Kawakami M, Horita S, Murakami K, Kirita T. Influence of bone parameters on peri-implant bone strain distribution in the posterior mandible. *Med Oral Patol Oral Cir Bucal* 2015;20:e66-73.
[PUBMED](#) | [CROSSREF](#)
20. Morton D, Jaffin R, Weber HP. Immediate restoration and loading of dental implants: clinical considerations and protocols. *Int J Oral Maxillofac Implants* 2004;19 Suppl:103-8.
[PUBMED](#)
21. Lekholm U, Zarb GA. Patient selection and preparation. In: Brånemark PI, Zarb GA, Albrektsson T, editors. *Tissue-integrated prostheses: osseointegration in clinical dentistry*. Chicago (IL): Quintessence; 1985. p.199-209.
22. Kurniawan D, Nor FM, Lee HY, Lim JY. Finite element analysis of bone-implant biomechanics: refinement through featuring various osseointegration conditions. *Int J Oral Maxillofac Surg* 2012;41:1090-6.
[PUBMED](#) | [CROSSREF](#)
23. Keyak JH, Rossi SA, Jones KA, Skinner HB. Prediction of femoral fracture load using automated finite element modeling. *J Biomech* 1998;31:125-33.
[PUBMED](#) | [CROSSREF](#)
24. Ding X, Liao SH, Zhu XH, Zhang XH, Zhang L. Effect of diameter and length on stress distribution of the alveolar crest around immediate loading implants. *Clin Implant Dent Relat Res* 2009;11:279-87.
[PUBMED](#) | [CROSSREF](#)
25. Mericske-Stern R, Assal P, Mericske E, Bürgin W. Occlusal force and oral tactile sensibility measured in partially edentulous patients with ITI implants. *Int J Oral Maxillofac Implants* 1995;10:345-53.
[PUBMED](#)
26. Hudieb M, Wakabayashi N, Suzuki T, Kasugai S. Morphologic classification and stress analysis of the mandibular bone in the premolar region for implant placement. *Int J Oral Maxillofac Implants* 2010;25:482-90.
[PUBMED](#)
27. Gonda T, Yasuda D, Ikebe K, Maeda Y. Biomechanical factors associated with mandibular cantilevers: analysis with three-dimensional finite element models. *Int J Oral Maxillofac Implants* 2014;29:e275-82.
[PUBMED](#)
28. Vandamme K, Naert I, Geris L, Vander Sloten J, Puers R, Duyck J. The effect of micro-motion on the tissue response around immediately loaded roughened titanium implants in the rabbit. *Eur J Oral Sci* 2007;115:21-9.
[PUBMED](#) | [CROSSREF](#)
29. Trisi P, Perfetti G, Baldoni E, Berardi D, Colagiovanni M, Scogna G. Implant micromotion is related to peak insertion torque and bone density. *Clin Oral Implants Res* 2009;20:467-71.
[PUBMED](#) | [CROSSREF](#)
30. Cha JY, Kil JK, Yoon TM, Hwang CJ. Miniscrew stability evaluated with computerized tomography scanning. *Am J Orthod Dentofacial Orthop* 2010;137:73-9.
[PUBMED](#) | [CROSSREF](#)
31. Shen WL, Chen CS, Hsu ML. Influence of implant collar design on stress and strain distribution in the crestal compact bone: a three-dimensional finite element analysis. *Int J Oral Maxillofac Implants* 2010;25:901-10.
[PUBMED](#)

32. Frost HM. Skeletal structural adaptations to mechanical usage (SATMU): 2. Redefining Wolff's law: the remodeling problem. *Anat Rec* 1990;226:414-22.
[PUBMED](#) | [CROSSREF](#)
33. Patten CA, Caler WE, Carter DR. Cyclic mechanical property degradation during fatigue loading of cortical bone. *J Biomech* 1996;29:69-79.
[PUBMED](#) | [CROSSREF](#)
34. Mellal A, Wiskott HW, Botsis J, Scherrer SS, Belser UC. Stimulating effect of implant loading on surrounding bone. Comparison of three numerical models and validation by in vivo data. *Clin Oral Implants Res* 2004;15:239-48.
[PUBMED](#) | [CROSSREF](#)
35. Huang HL, Fuh LJ, Hsu JT, Tu MG, Shen YW, Wu CL. Effects of implant surface roughness and stiffness of grafted bone on an immediately loaded maxillary implant: a 3D numerical analysis. *J Oral Rehabil* 2008;35:283-90.
[PUBMED](#) | [CROSSREF](#)
36. Ferreira MB, Barão VA, Delben JA, Faverani LP, Hipólito AC, Assunção WG. Non-linear 3D finite element analysis of full-arch implant-supported fixed dentures. *Mater Sci Eng C* 2014;38:306-14.
[PUBMED](#) | [CROSSREF](#)
37. Duaibis R, Kusnoto B, Natarajan R, Zhao L, Evans C. Factors affecting stresses in cortical bone around miniscrew implants: a three-dimensional finite element study. *Angle Orthod* 2012;82:875-80.
[PUBMED](#) | [CROSSREF](#)
38. Chiapasco M. Early and immediate restoration and loading of implants in completely edentulous patients. *Int J Oral Maxillofac Implants* 2004;19 Suppl:76-91.
[PUBMED](#)
39. Seker E, Ulusoy M, Ozan O, Doğan DÖ, Seker BK. Biomechanical effects of different fixed partial denture designs planned on bicortically anchored short, graft-supported long, or 45-degree-inclined long implants in the posterior maxilla: a three-dimensional finite element analysis. *Int J Oral Maxillofac Implants* 2014;29:e1-9.
[PUBMED](#) | [CROSSREF](#)
40. Chang PK, Chen YC, Huang CC, Lu WH, Chen YC, Tsai HH. Distribution of micromotion in implants and alveolar bone with different thread profiles in immediate loading: a finite element study. *Int J Oral Maxillofac Implants* 2012;27:e96-101.
[PUBMED](#)